Inorg. Chem. **2006**, *45*, 4468–4477

Metal and Ligand K-edge XAS of Titanium–TEMPO Complexes: Determination of Oxidation States and Insights into Ti–O Bond Homolysis

Serena DeBeer George,*,† Kuo-Wei Huang,‡ Robert M. Waymouth,*,‡ and Edward I. Solomon*,†,‡

Stanford Synchrotron Radiation Laboratory, SLAC, Stanford University, Stanford, California 94309, and Department of Chemistry, Stanford University, Stanford, California 94305

Received March 9, 2006

Ti–TEMPO (TEMPO = 2,2,6,6-tetramethylpiperidine-*N*-oxyl) provides a means for generating Ti(III) complexes by homolysis of the Ti–O bond. It has been determined that bis-Cp-Ti-TEMPO complexes readily undergo homolytic cleavage while the mono-Cp-Ti-TEMPO complexes do not. Here Ti K- and Cl K-edge XAS are applied to directly determine the oxidation state of $TiCl_3$TEMPO, $TiCpCl_2$TEMPO, and $TiCp_2$ClTEMPO, with reference to Ti(III) and Ti(IV) complexes of known oxidation state. The Ti K-edge data show that Ti(III) complexes exhibit a pre-edge feature ~1 eV lower than any of the Ti(IV) complexes; while the Cl K-edges show that Ti(III) complexes have a Cl K- pre-edge feature to ~1 eV higher energy than any of the Ti(IV) complexes. Taken together, the Ti and Cl K-edge data indicate that the Ti–TEMPO complexes are best described as Ti(IV)–TEMPO anions (rather than Ti(III)–nitroxyl radicals). In addition, the Cl K-edges indicate that replacement of Cl by Cp weakens the bonding with the remaining ligands, with the Cl 3p covalency decreasing from 25% to 21% to 17% on going from $TiCl_3$-TEMPO to $TiCpCl_2$TEMPO to $TiCp_2$ClTEMPO. DFT calculations also show that the electronic structures of the Ti–TEMPO complexes are modulated by the replacement of chloride by Cp. The effect of the Cp on the ancillary ligation is one factor that contributes to facile Ti–O bond homolysis in $TiCp_2$ClTEMPO. However, the results indicate the primary contribution to the energetics of Ti–O bond homolysis in $TiCp_2$ClTEMPO is stabilization of the three-coordinate product by Cp.

I. Introduction

Interest in organotitanium complexes stems from their prominent role as homogeneous catalysts, particularly as olefin polymerization catalysts.[1−4] The reactivity of titanium catalysts is frequently correlated with their local site symmetry or oxidation state,[5−7] and hence, the ability to fine-tune the geometric and electronic structure of these complexes has important implications for their catalytic behavior.

Recent work has shown that the reversible homolytic cleavage of weak Ti−O bonds derived from stable nitroxyl radical TEMPO (2,2,6,6-tetramethylypiperidine-*N*-oxyl) provides a means of reversibly generating Ti(III) complexes.[8] Experimental and theoretical studies reveal that the coordination geometries[7,9−12] and strength of the Ti−O bonds[8] derived from nitroxyl radicals depends sensitively on the ancillary ligation at titanium. In $TiCl_3$TEMPO, the TEMPO coordinates in an η^2 fashion through both the N and O atoms, while in the $TiCpCl_2$TEMPO complex, the TEMPO is coordinated

* To whom correspondence should be addressed. Email: serena@slac.stanford.edu (S.D.G.); waymouth@stanford.edu (R.M.W.); edward.solomon@stanford.edu (E.I.S.).

† Stanford Synchrotron Radiation Laboratory.

‡ Department of Chemistry.

(1) Alt, H. G.; Köppl, A. *Chem. Rev.* **2000**, *100*, 1205.
(2) Britzinger, H. H.; Fischer, D.; Mülhaupt, R.; Rieger, B.; Waymouth, R. M. *Angew. Chem.* **1995**, *34*, 1143.
(3) Coates, G. W. *Chem. Rev.* **2000**, *100*, 1223.
(4) Hlatky, G. G. *Coord. Chem. Rev.* **1999**, *181*, 243.
(5) Grassi, A.; Saccheo, S.; Zambelli, A.; Laschi, F. *Macromolecules* **1998**, *31*, 5588.
(6) Williams, E. F.; Murray, M. C.; Baird, M. C. *Macromolecules* **2000**, *33*, 261.
(7) Mahanthappa, M. K.; Waymouth, R. M. *J. Am. Chem. Soc.* **2001**, *123*, 12093.
(8) Huang, K.-W.; Han, J. H.; Cole, A. P.; Musgrave, C. B.; Waymouth, R. M. *J. Am. Chem. Soc.* **2005**, *127*, 3807.
(9) Mahanthappa, M. K.; Huang, K.-W.; Cole, A. P.; Waymouth, R. M. *Chem. Commun.* **2002**, 502.
(10) Huang, K.-W.; Waymouth, R. M. *J. Am. Chem. Soc.* **2002**, *124*, 8200.
(11) Mahanthappa, M. K.; Cole, A. P.; Waymouth, R. M. *Organometallics* **2004**, *23*, 1405.
(12) Mahanthappa, M. K.; Cole, A. P.; Waymouth, R. M. *Organometallics* **2004**, *23*, 836.

10.1021/ic060402t CCC: $33.50
Published on Web 04/19/2006

Scheme 1

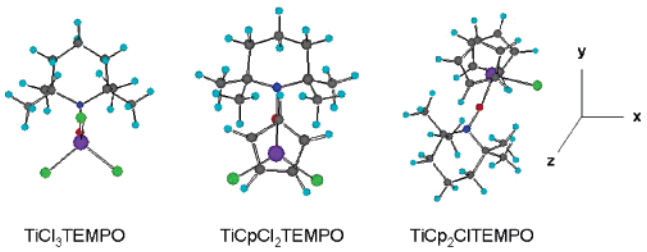

in an η^1 mode through the oxygen. The ancillary ligation also influences the thermal stability of these complexes. The bis-cyclopentadienyl complex $TiCp_2Cl(TEMPO)$ readily undergoes Ti−O bond homolysis at 60 °C, while the mono-cyclopentadienyl complex $TiCpCl_2(TEMPO)$ is thermally stable at 100 °C for days. Previous DFT calculations on these complexes have shown that replacement of an ancillary Cl ligand by the more strongly donating Cp ligand can weaken the Ti−O bond by up to 26 kcal/mol.[8] This was attributed to either destabilization of the Ti−O bond by ancillary ligation or preferential stabilization of the Ti(III) product; however, it is believed that the latter effect dominates due to the coordinatively and electronically unsaturated nature of Ti(III).

To obtain further insight into the electronic structure of these Ti−TEMPO complexes, we have initiated Ti and Cl K-edge X-ray absorption spectroscopic (XAS) studies on $TiCl_3TEMPO$, $TiCpCl_2TEMPO$, and $TiCp_2ClTEMPO$ (Cp = cyclopentadienyl) (Scheme 1), as well as representative Ti(III) complexes $TiCl_3$ and Cp^{tt}_2TiCl (Cp^{tt} = 1,3-di-tertbutylcyclopentadienyl).[8−12] Though there are examples of Ti(IV) XAS studies in the literature,[13−18] relatively few examples of Ti(III) XAS data are available[19,20] and to our knowledge, organometallic Ti(III) complexes have not been previously characterized by XAS. These studies develop a detailed understanding of the Ti 1s → 3d pre-edge transition and its sensitivity to changes in the oxidation state of the titanium. This is of particular interest for the Ti−TEMPO complexes since TEMPO could coordinate to Ti, forming either a Ti(III)−nitroxyl radical or a Ti(IV)−nitroxide complex (in which the TEMPO is reduced and serves as an anionic ligand). Crystal structures of $TiCl_3TEMPO$ and $TiCpCl_2TEMPO$ indicate that the N−O bond length is most consistent with the Ti(IV)−TEMPO anion;[9] however, this assignment is based on structure alone and a more detailed electronic structural description is warranted. XAS results are used to experimentally describe the electronic structure

Scheme 2

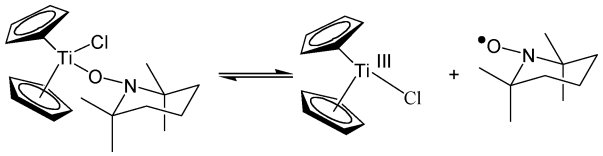

of the Ti−TEMPO complexes. These results also serve to illustrate the utility of Ti and Cl K-edge XAS as indicators of oxidation state for titanium complexes.

In addition to oxidation state, the nature of the Ti−TEMPO bond and the factors which contribute to the facile homolytic cleavage of Ti−O bonds derived from nitroxyl radicals can be addressed by XAS. Ti K- and Cl K-edge XAS combined with DFT studies on the Ti−TEMPO complexes, as well as on $Ti(III)(^{tt}Cp)_2Cl$ (^{tt}Cp = η^5-1,3-di-*tert*-butyl-cyclopentadienyl), allow us to examine these issues experimentally and provides a reference for understanding Ti−O bond cleavage. Ti K-edge provides both a direct measure of oxidation state and a measure of 4p mixing with the 3d orbitals, which reflects covalent interactions with ligands and allows for evaluation of DFT results.[18] Cl K-edge XAS provides a direct measure of Cl 3p character in the unoccupied Ti 3d orbitals and thus provides an experimental measure of the effect of the ancillary ligation[18,21] and further verification of DFT results. Together the Ti and Cl XAS data and DFT calculations give a detailed description of the electronic structure of the Ti−TEMPO complexes and allow for a molecular orbital description of the Ti−TEMPO bonding in both the η^1 and η^2 modes. The electronic structure descriptions of $TiCp_2ClTEMPO$ (the "reactant" in the homolysis reaction, Scheme 2) and $Ti(III)(^{tt}Cp)_2Cl$ (which approximates the homolysis "product") are of particular interest. By coupling experimental data with calculations, we are able to gain further insight into the influence of the ancillary Cp ligands and the factors that govern Ti−O bond homolysis. The energetics of both homolytic (Ti(III)) and heterolytic (Ti(IV)) reaction paths are examined through DFT calculations and provide insight into the importance of the oxidation state and coordination number of titanium in the reaction pathway. In addition, an estimate of the relative energetic contributions of spin polarization and reduced charge separation in the homolytic cleavage reaction is obtained.

II. Experimental Section

A. Sample Preparation. α-$TiCl_3$ was purchased from Strem Chemicals (Newburyport, MA) and was used without further purification. $Ti(^{tt}Cp)_2Cl$, $TiCl_3TEMPO$, $TiCpCl_2TEMPO$, and $TiCp_2ClTEMPO$ were prepared according to published procedures.[9,22] All samples were prepared in an inert-atmosphere glovebox and were measured as solids. For Ti K-edge measurement, solids were diluted with graphite (which had been stirred in hot HCl, washed with ethanol, and dried in vacuo) and pressed into 0.5-mm-thick Al spacers sealed with 38-μm Kapton windows. For Cl K-edge measurements, solid samples were ground into a fine powder and dispersed as thinly as possible on Mylar tape.

(13) Fraile, J. M.; García, J.; Mayoral, J. A.; Proietti, M. G.; Sánchez, M. C. *J. Phys. Chem.* **1996**, *100*, 19484.
(14) Farges, F.; Brown, G. E., Jr.; Rehr, J. J. *Phys. Rev. B* **1997**, *56*, 1809.
(15) Matsuo, S.; Sakaguchi, N.; Obuchi, E.; Nakano, K.; Perera, R. C. C.; Watanabe, T.; Matsuo, T.; Wakita, H. *Anal. Sci.* **2001**, *17*, 149.
(16) Wasserman, E. P.; Westwood, A. D.; Zhengtian, Y.; Oskam, J. H.; Duenas, S. L. *J. Mol. Catal. A* **2001**, *172*, 67.
(17) Shirley, E. *J. Elect. Spec.* **2004**, *136*, 77.
(18) DeBeer George, S.; Brant, P.; Solomon, E. I. *J. Am. Chem. Soc.* **2005**, *127*, 667.
(19) Miyanaga, T.; Watanabe, I.; Ikeda, S. *Bull. Chem. Soc. Jpn.* **1990**, *63*, 3282.
(20) Léon, A.; Kircher, O.; Jörg, R.; Fitchner, M. *J. Phys. Chem. B* **2004**, *108*, 16372.
(21) Glaser, T.; Rose, K.; Shadle, S. E.; Hedman, B.; Hodgson, K. O.; Solomon, E. I. *J. Am. Chem. Soc.* **2001**, *123*, 442.
(22) King, W. A.; Di Bella, S.; Gulino, A.; Lanza, G.; Fragala, I. L.; Stern, C. L.; Marks, T. J. *J. Am. Chem. Soc.* **1999**, *121*, 355.

B. X-ray Absorption Spectroscopy and Measurements and Data Analysis. All data were measured at the Stanford Synchrotron Radiation Laboratory under ring conditions of 3.0 GeV and 60−100 mA. Data were measured using the 54-pole wiggler beam line 6-2 in high-magnetic-field mode of 10 kG with a Ni-coated harmonic rejection mirror and a fully tuned (5366 eV for the Ti K-edge and 3150 eV for the Cl K-edge) Si(111) double-crystal monochromator. Details of the optimization of this setup for low-energy studies have been described previously.[23]

i. Ti K-Edges. All Ti K-edge measurements were made at room temperature and measured as transmission spectra. To check for reproducibility, 2−3 scans were measured for all samples. The energy was calibrated from Ti foil spectra run at intervals between sample scans. The first inflection point of the Ti foil was fixed at 4966.0 eV. A step size of 0.11 eV was used over the edge region. Data were measured from 4700 to 5370 eV. Data were averaged, and a smooth background was removed from all spectra by fitting a polynomial to the pre-edge region and subtracting this polynomial from the entire spectrum. Normalization of the data was accomplished by fitting a flattened polynomial or straight line to the post-edge region and normalizing the edge jump to 1.0 at 5000 eV. Fits to the edges were performed using the program EDG_FIT.[24] Second-derivative spectra were used as guides to determine the number and position of peaks. Pre-edge and rising edge features were modeled by pseudo-Voigt line shapes. For the pre-edge feature, a fixed 1:1 ratio of Lorentzian to Gaussian contributions was used. All fits were performed over three energy ranges: 4963−4974, 4963−4975, and 4963−4976 eV. The reported intensity values are based on the average of all good fits. Normalization procedures can introduce ∼3% error in pre-edge peak intensities in addition to the error resulting from the fitting procedure.

ii. Cl K-Edges. All Cl K-edge measurements were made at room temperature and measured as fluorescence spectra using a Lytle detector.[25,26] To check for reproducibility, 2−3 scans were measured for each of the solid samples. The energy was calibrated from D_{2d}-$[Cs_2CuCl_4]$ spectra run at intervals between sample scans. The maximum of the first pre-edge feature in the spectrum was fixed at 2820.20 eV. A step size of 0.07 eV was used over the edge region. Data were measured from 2720 to 3150 eV. Data were averaged, and a smooth background was removed from all spectra by fitting a polynomial to the pre-edge region and subtracting this polynomial from the entire spectrum. Normalization of the data was accomplished by fitting a flattened polynomial or straight line to the post-edge region and normalizing the edge jump to 1.0 at 2840 eV. Fits to the Cl K-edge data were performed over three energy ranges: 2817−2826, 2817−2827, and 2817−2828 eV. The reported intensity values are based on the average of all good fits. Normalization procedures can introduce ∼3% error in pre-edge peak intensities in addition to the error resulting from the fitting procedure.

C. Electronic Structure Calculations. Density functional calculations (BP86) were carried out using ADF2000 on a Silicon Graphics Origin 2000 multiprocessor computer.[27,28] A triple-ζ Slater-type orbital basis set (ADF basis set V) with a single polarization function at the local density approximation of Vosko, Wilk, and Nusair[29] and the nonlocal gradient corrections of Becke[30] and Perdew[31] were employed. The crystal structures of $Ti(^{tt}Cp)_2Cl$,[32] $TiCl_3TEMPO$,[9] and $TiCpCl_2TEMPO$[9] were used as initial input models for the geometry optimizations (the coordinate system is given in Scheme 1). No symmetry was imposed for geometry optimizations. The optimized coordinates are provided in the Supporting Information.

III. Results and Analysis

A. Ti K-Edge XAS. Figure 1 shows a comparison of the normalized Ti K-pre-edge XAS spectra (left) of Ti(III) complexes ($TiCl_3$ and $Ti(^{tt}Cp)_2Cl$, top), Ti(IV) complexes ($TiCl_4$, $TiCpCl_3$, and $TiCp_2Cl_2$, center), and the Ti−TEMPO complexes ($TiCl_3TEMPO$, $TiCpCl_2TEMPO$, and $TiCp_2ClTEMPO$, bottom). The corresponding second derivatives are shown on the right. Data over the full edge region are provided in the Supporting Information (Figure S1). All of the complexes exhibit a pre-edge feature between 4966 and 4970 eV, corresponding to a 1s → 3d transition, which is electric dipole forbidden but can gain intensity through metal 3d−4p mixing. The second derivatives over the pre-edge region clearly show that the Ti(III) complexes (Figure 1, top) exhibit a feature ∼1 eV lower in energy than any of the Ti(IV) complexes (negative feature in the second derivative corresponds to a peak in the absorption). The much weaker pre-edge intensity in $TiCl_3$ is consistent with the octahedral geometry of this complex. In contrast, the Ti(IV) complexes (Figure 1, center) exhibit no pre-edge feature lower than ∼4968 eV. The change in pre-edge intensity and energy distribution in the Ti(IV) complexes in Figure 1, center, have been previously analyzed in detail.[18] The decrease in intensity on going from $TiCl_4$ to $TiCpCl_3$ to $TiCp_2Cl_2$ is due to the strong bonding interactions of the Cp ligands which have an interference effect with the configuration−interaction (CI)-induced mechanism of 3d−4p mixing. Inspection of the Ti−TEMPO pre-edges and second derivatives (Figure 1, bottom) show a trend which closely parallels that of the Ti(IV) complexes. The pre-edge transitions are in the 4968−4969 eV range, indicating an oxidation state assignment consistent with Ti(IV). In addition, the decrease in pre-edge intensity upon replacement of Cl by Cp parallels that of the Ti(IV) complexes, suggesting a similar interference mechanism of the Cp with CI-induced 3d−4p mixing. The decrease in pre-edge intensity shows a linear correlation with the decrease in 3d−4p mixing predicted by DFT calculations (Table 1 and section III.C.).

B. Cl K-Edge XAS. Figure 2 shows a comparison of the normalized Cl K-edge spectra for Ti(III) complexes ($TiCl_3$ and $Ti(^{tt}Cp)_2Cl$, top), Ti(IV) complexes ($TiCl_4$, $TiCpCl_3$, and $TiCp_2Cl_2$, center), and the Ti−TEMPO complexes ($TiCl_3$-TEMPO, $TiCpCl_2TEMPO$, and $TiCp_2ClTEMPO$, bottom). The pre-edge features in the Cl K-edge spectra correspond

(23) Hedman, B.; Frank, P.; Gheller, S. F.; Roe, A. L.; Newton, W. E.; Hodgson, K. O. *J. Am. Chem. Soc.* **1988**, *110*, 3798.
(24) George, G. N., Stanford Synchrotron Radiation Laboratory, Stanford Linear Accelerator Center, Stanford University, Stanford, CA 94309.
(25) Lytle, F. W.; Greegor, R. B.; Sandstrom, D. R.; Marques, E. C.; Wong, J.; Spiro, C. L.; Huffman, G. P.; Huggins, F. E. *Nucl. Instrum. Methods* **1984**, *226*, 542.
(26) Stern, E. A.; Heald, S. M. *Rev. Sci. Instrum.* **1979**, *50*, 1579.
(27) te Velde, G.; Bickelhaupt, F. M.; Baerends, E. J.; Guerra, C. F.; van Ginsberg, S. J. A.; Snijders, J. G.; Ziegler, T. *J. Comput. Chem.* **2001**, *22*, 931.
(28) Baerends, E. J.; Ellis, D. E.; Ros, P. *Chem. Phys.* **1973**, *2*, 41.
(29) Vosko, S. H.; Wilk, L.; Nusair, M. *Can. J. Phys.* **1980**, *58*, 1200.
(30) Becke, A. D. *Phys. Rev. A* **1988**, *38*, 3098.
(31) Perdew, J. P. *Phys. Rev. B* **1986**, *33*, 8822.
(32) Urazowski, I. F.; Ponomaryov, V. I.; Ellert, O. G.; Nifant'ev, I. E.; Lemenovskii, D. A. *J. Organomet. Chem.* **1988**, *356*, 181.

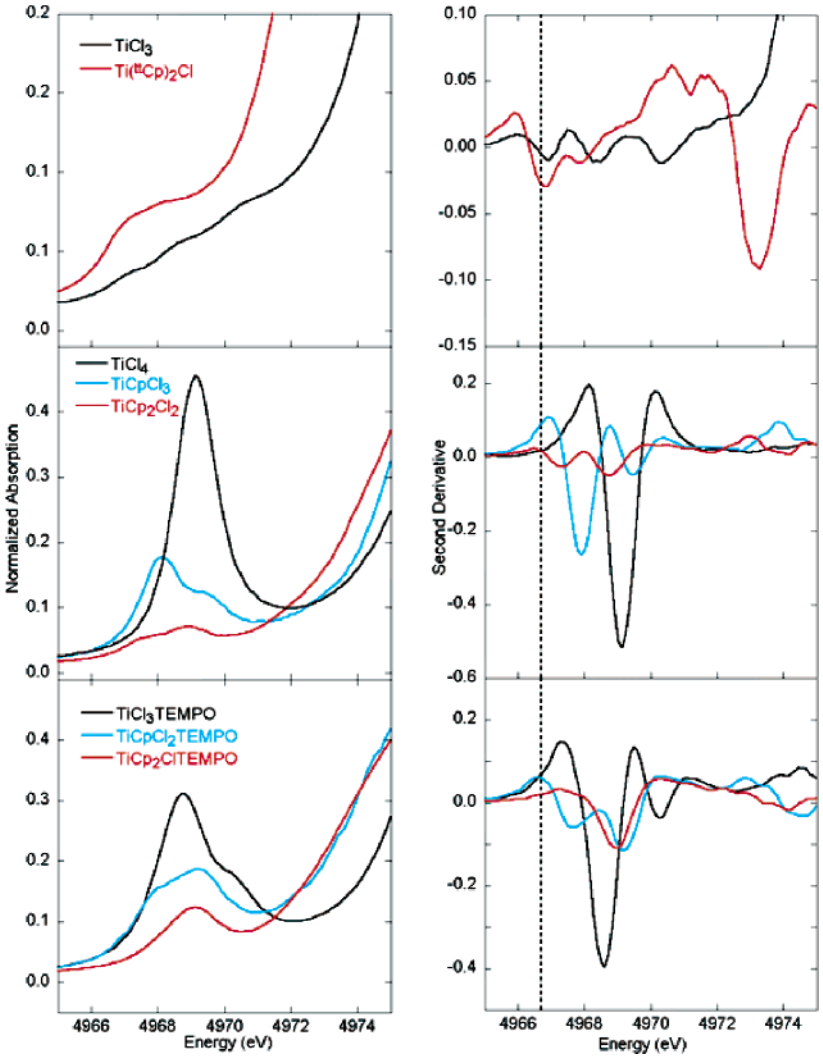

Figure 1. Normalized Ti K-pre-edge spectra (left) and corresponding second derivatives (right) of Ti(III) complexes ($TiCl_3$ and $Ti(^{tt}Cp)_2Cl$, top), Ti(IV) complexes ($TiCl_4$, $TiCpCl_3$, and $TiCp_2Cl_2$, center), and the Ti−TEMPO complexes ($TiCl_3$TEMPO, $TiCpCl_2$TEMPO, and $TiCp_2Cl$TEMPO, bottom).

Table 1. Comparison of Ti K- and Cl K-Pre-Edge XAS Intensities and DFT Calculated Values

	Ti K-pre-edge intensity[a]	exptl[b] %4p	calcd %4p	Cl K-pre-edge intensity[a]	exptl %Cl 3p[c]	calcd %Cl 3p[c]
$TiCl_3$TEMPO	62.8 (2.1)	12.5	8.3	2.33 (0.15)	33	25
$TiCpCl_2$TEMPO	36.5 (3.2)	6.6	4.3	1.74 (0.14)	25	21
$TiCp_2Cl$TEMPO	18.8 (0.5)	2.8	1.7	1.54 (0.10)	22	17
$Ti(^{tt}Cp)_2Cl$	14.8 (1.2)	1.9	1.3	1.62 (0.11)	24	22

[a] For consistency with previous publications, metal K-edge intensities are multiplied by 100 while ligand K-edge intensities are not. Error in intensity is given in parentheses. [b] Determined using linear correlation between pre-edge intensity and 4p mixing from ref 18. [c] The percent Cl 3p character is reported per Ti−Cl bond.

to transitions from the Cl 1s orbitals to the unoccupied molecular orbitals formed by interaction of the Cl 3p and Ti 3d orbitals, while the rising edge corresponds to a Cl 1s to Cl 4p transition. If we make the reasonable assumption that Cl 4p orbital energy is relatively unaffected by changes in Z_{eff}, we can use the edge energy to estimate the Cl 1s energy shifts and their effects on the 1s-to-3d pre-edge energies. Comparison of the known Ti(III) and Ti(IV) complexes shows that the unoccupied Ti 3d orbitals are ∼1 eV higher in energy in the Ti(III) complexes, consistent with the lower effective nuclear charge. Comparison of the Cl K-pre-edge and rising edge energies of the Ti−TEMPO complexes (Figure 2, bottom) to those of the known Ti(III) (top) and Ti(IV) (center) complexes clearly shows that the TEMPO data are most consistent with the Ti(IV) oxidation state, further supporting the assignment from the Ti K-edge.

There is also a clear change in the Cl K-edge total pre-edge intensity (both in amplitude and in the energy separation of the pre-edge peaks) which decreases on going from $TiCl_3$-TEMPO to $TiCpCl_2$TEMPO to $TiCp_2Cl$TEMPO (Table 1). The decrease in intensity reflects a weakening of the remaining Ti−Cl bond(s) upon replacement of a chloride by Cp. Using D_{2d}-$Cs_2[CuCl_4]$ as a well-defined reference with 7.5% Cl 3p character per Cu−Cl bond,[33−35] the Cl 3p character per Ti−Cl bond can be determined for each of the Ti−TEMPO complexes. Using the experimentally deter-

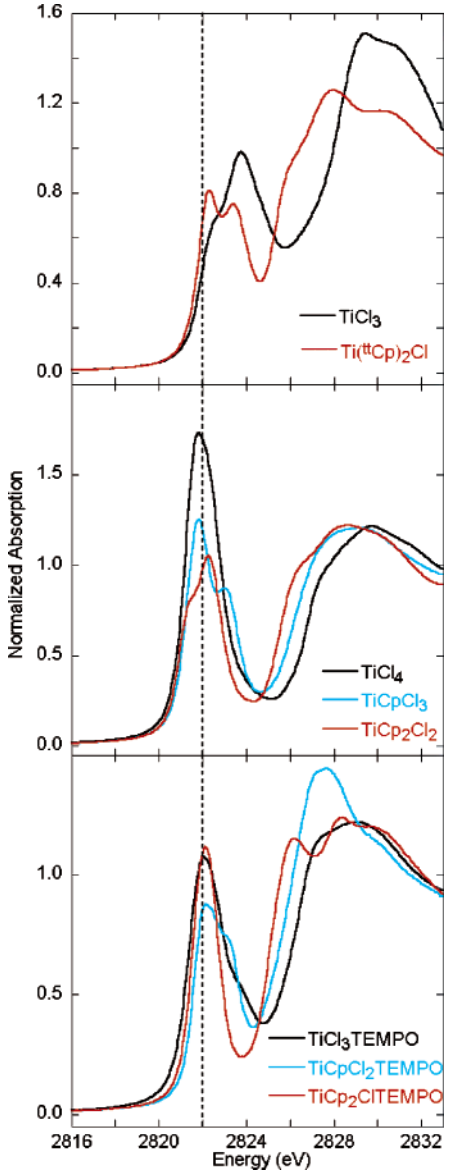

Figure 2. Normalized Cl K-pre-edge spectra of Ti(III) complexes ($TiCl_3$ and $Ti(^{tt}Cp)_2Cl$, top), Ti(IV) complexes ($TiCl_4$, $TiCpCl_3$, and $TiCp_2Cl_2$, center), and the Ti−TEMPO complexes ($TiCl_3$TEMPO, $TiCpCl_2$TEMPO, and $TiCp_2Cl$TEMPO, bottom).

mined pre-edge intensities, the Cl 3p character per Ti−Cl bond is 33%, 25%, and 22% for $TiCl_3$TEMPO, $TiCpCl_2$-TEMPO, and $TiCp_2Cl$TEMPO, respectively. These are consistent with the trends observed in the DFT calculations (Table 2 and section III.C.), which also show that the addition of the Cp ligand weakens the Ti−Cl bond and parallels the trends previously observed for $TiCl_4$, $TiCpCl_3$, and $TiCp_2Cl_2$.[36] This is consistent with crystallographic results which show that the Ti−Cl bond length increases from 2.22 to 2.28 to 2.53 Å on going from $TiCl_3$TEMPO, $TiCpCl_2$TEMPO, and $TiCp_2Cl$(4-MeO-TEMPO), respectively.[8,9]

Table 2. Results of ADF Calculations for the Five Metal d-based Orbitals in $TiCl_3$TEMPO, $TiCpCl_2$TEMPO, and $TiCp_2Cl$TEMPO

$TiCl_3$TEMPO						
MO label	81A	82A	83A	84A	85A	total
energy (eV)	−3.407	−3.345	−2.856	−2.813	−1.362	
			orb contribution			
Ti d total	75.93	78.92	74.48	70.77	66.22	366.32
Ti 4p	1.44	0.72	2.37	2.97	0.79	8.29
Cl p	16.97	13.95	14.26	18.56	11.22	74.96
TEMPO	3.27	5.81	5.47	4.77	20.52	39.84
$TiCpCl_2$TEMPO						
MO label	90A	91A	92A	93A	94A	
energy (eV)	−3.015	−2.484	−2.254	−1.631	−1.449	
			orb contribution			
Ti d total	72.88	70.03	70.75	70.07	61.23	344.96
Ti 4p	0.91	0.18	0.26	0.47	2.46	4.28
Cl p	15.15	8.25	4.49	11.32	3.45	42.66
TEMPO	0.58	11.27	17.04	0.13	15.89	44.91
Cp	6.43	8.34	4.39	20.06	16.01	55.23
$TiCp_2Cl$TEMPO						
MO label	99A	100A	101A	102A	103A	
energy (eV)	−2.490	−2.115	−1.862	−1.824	−1.415	
			orb contribution			
Ti d total	69.33	71.23	69.01	70.86	64.85	345.28
Ti 4p	0.12	0.36	0.22	0.18	0.85	1.73
Cl p	5.38	2.20	6.45	2.57	0.27	16.87
TEMPO, N	11.79	3.76	2.32	2.62	10.91	31.40
Cp	9.82	19.82	21.77	23.65	22.56	97.62

C. Electronic Structure Calculations. Ground-state DFT calculations have been used to obtain electronic structure descriptions of the Ti−TEMPO complexes. Both spin-restricted and spin-unrestricted calculations were performed. The spin-unrestricted calculation were allowed to polarize but showed no evidence for spin-polarization and gave results very similar to the spin-restricted calculations. The geometry-optimized results are generally in good agreement with the crystal structures of $TiCl_3$TEMPO, $TiCpCl_2$TEMPO, and $TiCp_2Cl$TEMPO(OMe) with differences of less than 0.04 Å in bond length and 3° in angle for all but the Ti−Cl distance in $TiCp_2Cl$TEMPO.[37] The results for all three Ti−TEMPO complexes are most consistent with Ti(IV) bound to a TEMPO anion, based on both the charge on the TEMPO (−0.7) and the TEMPO N−O bond lengths (1.40−1.42 Å). These results indicate that one electron has been transferred from the metal to the ligand and is consistent with the experimental Ti(IV) oxidation state assignment (section III.A.). Since in the XAS experiment the pre-edges probe the unoccupied d orbitals, which are a reflection of the uncompensated bonding densities, here we focus on the molecular orbitals which are directly correlated to our experimental results. The molecular orbital energy level diagrams for the 5-unoccupied metal valence orbitals of

(33) Shadle, S. E.; Hedman, B.; Hodgson, K. O.; Solomon, E. I. *J. Am. Chem. Soc.* **1995**, *117*, 2259.
(34) Gewirth, A. A.; Cohen, S. L.; Schugar, H. J.; Solomon, E. I. *Inorg. Chem.* **1987**, *26*, 1133.
(35) Didziulis, S. V.; Cohen, S. L.; Gewirth, A. A.; Solomon, E. I. *J. Am. Chem. Soc.* **1988**, *110*, 250.

(36) It is of interest to note that the Ti−Cl bonds are all slightly less covalent in the Ti−TEMPO series than in the corresponding $TiCl_4$, $TiCpCl_3$, and $TiCp_2Cl_2$ series (37%, 32%, and 25% per Ti−Cl bond, respectively). This reflects the increased donation of TEMPO relative to chloride.
(37) The calculated Ti−Cl bond length is ~0.13 Å shorter (2.40 vs 2.53 Å calculated) than in the crystal structure of $TiCp_2Cl$TEMPO(OMe). Geometry-optimized structures of both $TiCp_2Cl$TEMPO(OMe) and $TiCp_2Cl$TEMPO give similar results, ref 8.

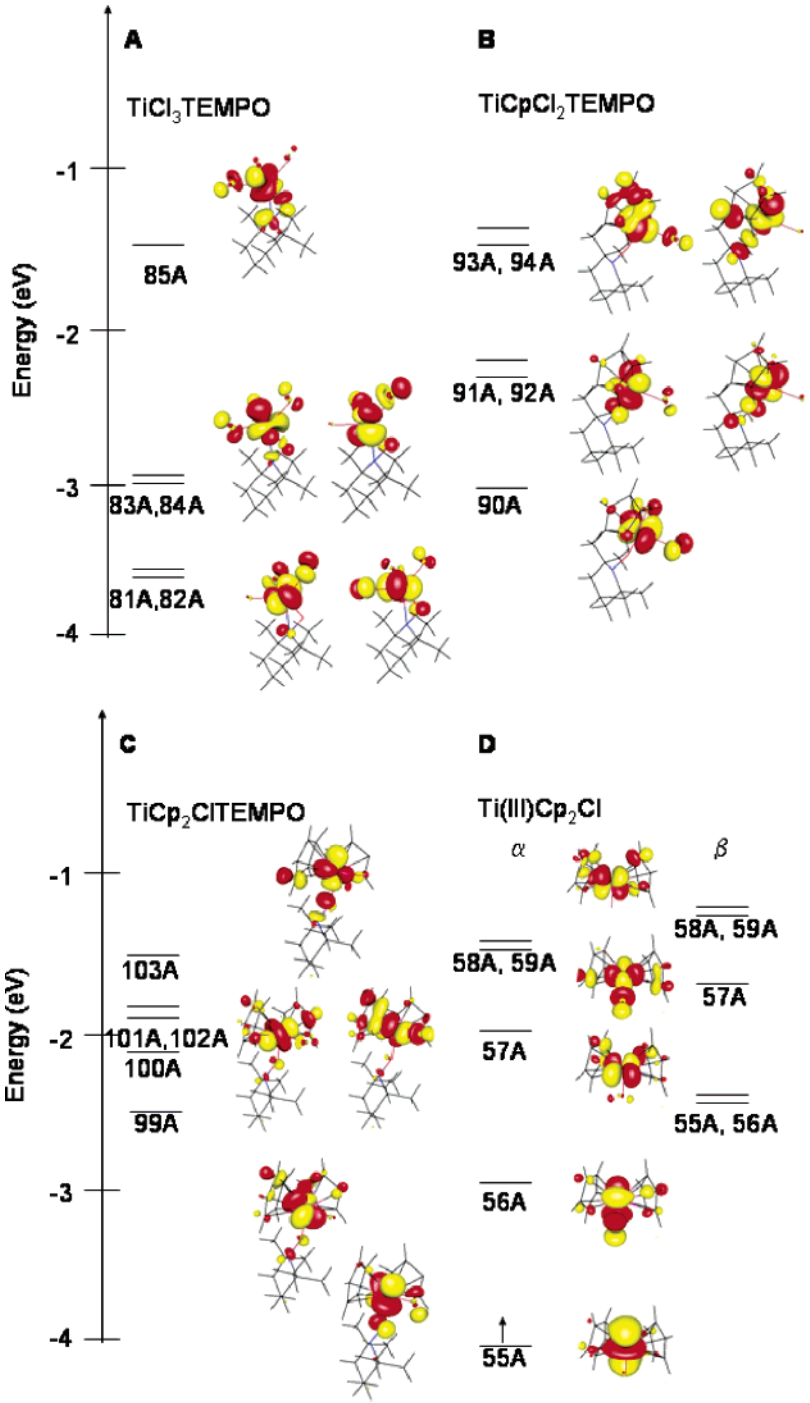

Figure 3. Molecular orbital energy level diagrams for the five metal d-based orbitals of $TiCl_3TEMPO$ (A), $TiCpCl_2TEMPO$ (B), $TiCp_2ClTEMPO$ (C), and $Ti(Cp)_2Cl$ (D). For $Ti(Cp)_2Cl$, contours are shown only for the spin-up orbitals.

$TiCl_3TEMPO$, $TiCpCl_2TEMPO$, and $TiCp_2ClTEMPO$ are show in Figure 3A−C, with the corresponding orbital compositions summarized in Table 2.

The DFT calculations clearly show that the TEMPO anion is a good donor to titanium (Table 2). TEMPO has two valence orbitals which are primarily involved in bonding to the titanium 3d orbitals (with small contributions from lower lying valence orbitals), the in-plane π HOMO-1 and the out-of-plane π HOMO, as shown in Figure 4A−B.

In η^2-$TiCl_3TEMPO$, there is ~40% TEMPO character in the 5-unoccupied d orbitals (Table 2). The bonding is dominated by a σ-type interaction between a Ti d orbital and the out-of-plane π HOMO of TEMPO (Figure 4C), raising this orbital to higher energy (Figure 3A, MO 85A). Smaller contributions from both the HOMO and HOMO-1 of TEMPO are present in the remaining d orbitals. All five d orbitals have significant Cl 3p contributions (11−19%, Table 2) and measurable Ti 4p contributions (0.7−3.0%).

On going to an η^1-bonding mode in $TiCpCl_2TEMPO$, the Ti−O−N bond angle increases to 156° (from 59° in η^2-$TiCl_3$-TEMPO) in allowing for a more a π-type interaction with the TEMPO out-of-plane HOMO with the Ti d orbital in

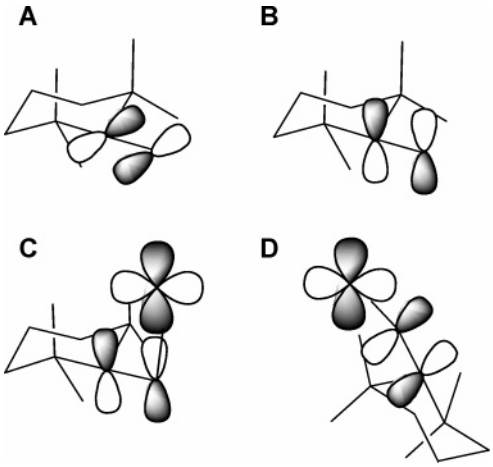

Figure 4. In-plane π HOMO-1 (A) and out-of-plane π HOMO (B) of TEMPO. The σ- (C) and π-type (D) interaction of the HOMO of TEMPO with the Ti d orbital.

MO 92A, Figures 3B and 4D. The in-plane HOMO-1 of TEMPO dominantly contributes to MO 91A, and significant contributions from lower lying valence orbitals of TEMPO (HOMO-2 and HOMO-3) are made to MO 94A. The total TEMPO contribution to the d orbitals increases slightly (from 40% in $TiCl_3$TEMPO) to 45% (Table 2), consistent with the 0.09 Å decrease in Ti−O bond length. In addition, there is a large contribution from the Cp ligand which interacts dominantly with MOs 93A and 94A (Figure 3B) raising these orbitals to higher energy. The Cl 3p character (per Cl ligand) has decreased relative to $TiCl_3$TEMPO (from ∼25% per Cl to ∼21% per Cl), consistent with the presence of other strongly donating ligands. The total Ti 4p contribution to the five metal d orbitals has also decreased from 8.3% to 4.3%, and may be attributed to an interference effect of the Cp with the CI induced 3d−4p mixing, as previously observed for Ti−Cp complexes.[18]

In the η^1-$TiCp_2ClTEMPO$ complex, the presence of an additional Cp leads to a slightly more bent Ti−O−N angle (∼145°), resulting in a more σ-type interaction with the HOMO of TEMPO and a decrease in the total TEMPO contribution to the five d orbitals. The out-of-plane HOMO of TEMPO contributes dominantly to MO 103A (Figure 3C), while the in-plane HOMO-1 contributes primarily to MO 99A. Overall, the total TEMPO contribution has decreased relative to the mono-Cp-TEMPO complex (from 45% in the mono-Cp-TEMPO to 31% in the bis-Cp-TEMPO). This may be attributed to the presence of an additional strong Cp donor ligand. The Cp ligands make significant contributions to all five metal d orbitals, decreasing the contribution of both the TEMPO and the remaining Cl ligands (from 21% per Cl ligand to 17% per Cl, in the mono- and bis-Cp-TEMPOs, respectively). In addition, the metal 4p contribution has also decreased further from 4.3% in mono-Cp TEMPO to 1.7% in bis-Cp-TEMPO.

Spin-unrestricted calculations have also been carried for $Ti(^{tt}Cp)_2Cl$ and $Ti(Cp)_2Cl$, where the latter is the product of $TiCp_2ClTEMPO$ homolysis. The geometry-optimized structures of $Ti(^{tt}Cp)_2Cl$ and $Ti(Cp)_2Cl$ are essentially identical

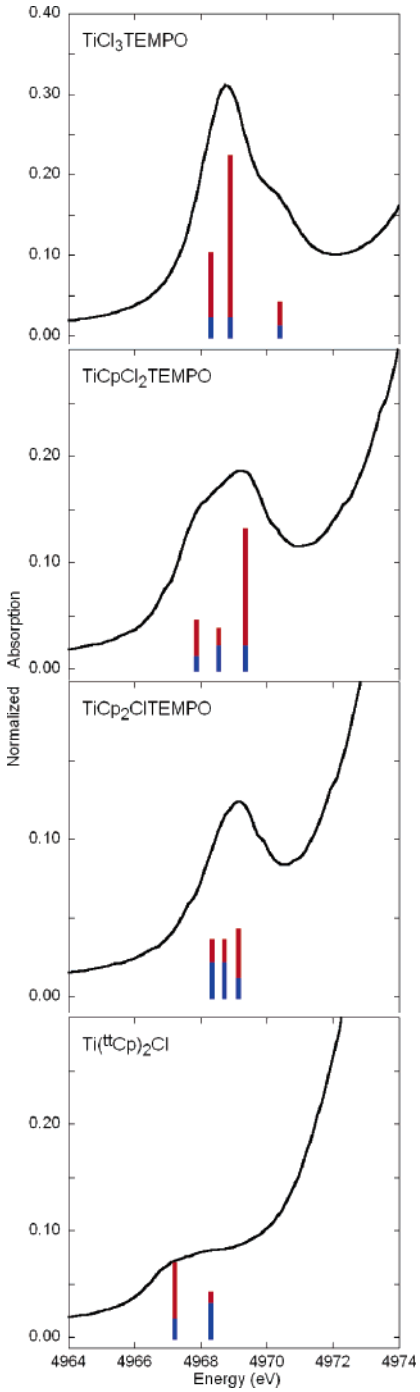

Figure 5. Comparison of Ti K-edge data to DFT-predicted splittings and intensities. Quadrupole contributions are shown in blue. Dipole contributions are shown in red.

in terms of structure and orbital contributions, and therefore, only the $Ti(Cp)_2Cl$ results are described.

The molecular orbital energy level diagram for the spin-up (α) and spin-down (β) orbitals is shown in Figure 3D. The Cp ligands contribute 81% and 57% to the unoccupied metal d-based α and β orbitals, respectively. In addition, there is an 8% Cp contribution to the lowest-energy occupied α orbital (MO 55A) due to back-bonding with the unoccupied e_2 (LUMO and LUMO+1) orbitals of the Cp ligands. The Cl ligand contributes 21% Cl 3p character, an increase relative to the bis-Cp-TEMPO complex (17% Cl 3p, Table

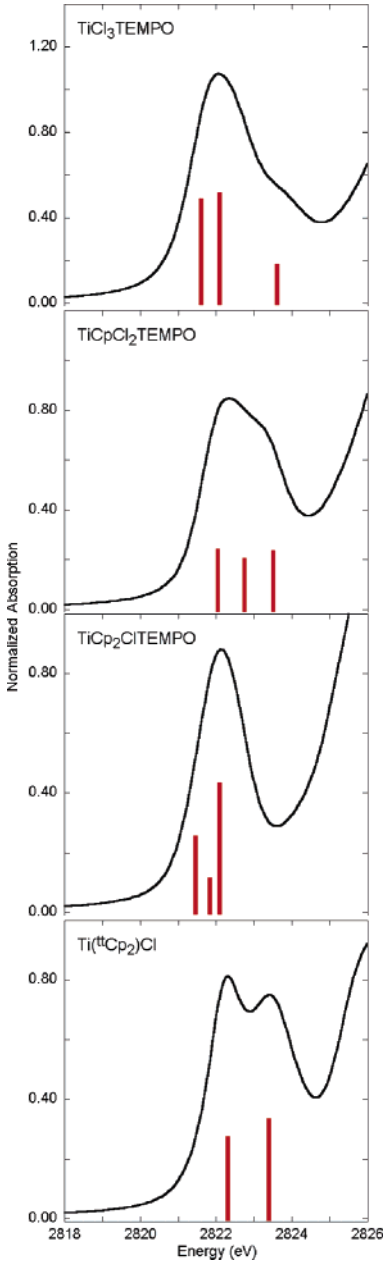

Figure 6. Comparison of Cl K-edge data to DFT predicted splittings and intensities.

2), which is consistent with a decrease in coordination number. Similar to the bis-Cp-TEMPO complex, the total 4p mixing over the unoccupied d orbitals is low, summing to ∼1.3% (Table 1).

D. Correlation to Spectral Data. To use the DFT results on the Ti−TEMPO and the $Ti(Cp)_2Cl$ complexes to obtain further insight into the electronic structure and reactivity, it is first important to establish that the DFT results reproduce our experimental data. Figures 5 and 6 show comparisons the DFT-predicted splittings and intensities to the experimental data for both the Ti K- and Cl K-edges, respectively. For the Ti K-edge data, a quadrupole contribution of 1.2 units per d orbital was assumed, as determined previously.[18] The remaining intensity is then assigned as 4p character. Using the linear relationship between experimental pre-edge intensity and DFT calculated 3d−4p mixing derived in ref 18, our experimental intensities should correspond to 12.5%, 6.6%, 2.8%, and 1.9% 4p mixing into the unoccupied 3d orbitals for $TiCl_3$TEMPO, $TiCpCl_2$TEMPO, $TiCp_2Cl$TEMPO, and $Ti(^{tt}Cp)_2Cl$, respectively (Table 1, exptl %4p). These values clearly parallel the trends obtained in the calculations, which show 8.3%, 4.3%, 1.7%, and 1.3% 3d−4p mixing for $TiCl_3$TEMPO, $TiCpCl_2$TEMPO, $TiCp_2Cl$TEMPO, and $Ti(Cp)_2Cl$, respectively (Table 1, calcd %4p). The energy splittings are based on relative d orbital distributions from the DFT calculations. Both the energy splittings and intensity distributions show very good agreement with experiment.

The Cl K-edge data were similarly correlated to DFT results (Figure 6). From calculations, the total Cl 3p character over the unoccupied metal d orbitals is 25%, 21%, 17%, and 22% per Ti−Cl bond (Table 1) for $TiCl_3$TEMPO, $TiCpCl_2$-TEMPO, $TiCp_2Cl$TEMPO, and $Ti(Cp)_2Cl$, respectively. This parallels the trend observed experimentally, which gave values of 33%, 25%, 22%, and 24% for $TiCl_3$TEMPO, $TiCpCl_2$TEMPO, $TiCp_2Cl$TEMPO, and $Ti(^{tt}Cp)_2Cl$, respectively (Figure 2, bottom, and Table 1). The stick plots shown in Figure 6 also demonstrate that the experimental energy and intensity distributions are well reproduced by the calculations. It should be noted that each individual contribution predicted by the DFT calculations is not necessarily resolved as a separate peak in the fits to the data.

IV. Discussion

The good agreement between the Ti K- and Cl K-edge data and the DFT-predicted results indicates that the calculations model the electronic structure well and may be used to aid in further interpretation of the electronic structure and reactivity.

A. Nature of the Ti−TEMPO Bond and Contribution of the Cp Ligands. The DFT calculations clearly show that all of the Ti−TEMPO systems are best described as Ti(IV)−TEMPO anion complexes. The TEMPO anion is a good donor to titanium, which dominantly bonds to the Ti 3d orbital via the in-plane π (HOMO-1) and out-of-plane π (HOMO) orbitals of TEMPO. In η^2-$TiCl_3$TEMPO, the bonding is dominated by a σ-type interaction with the out-of-plane π HOMO of TEMPO (Figure 4C) and a smaller contribution from an in-plane π-interaction with the HOMO-1. On going to an η^1-bonding mode in $TiCpCl_2$TEMPO, the increased Ti−O−N bond angle allows for a more a π-type interaction with the TEMPO out-of-plane π HOMO (Figure 4D) and results in an increase in the total TEMPO contribution to the d orbitals. Addition of another Cp in η^1-$TiCp_2$-ClTEMPO decreases the Ti−O−N angle (from 156° to 145°), resulting in a more σ-type interaction with the HOMO of TEMPO and a decrease in the total TEMPO contribution to the five d orbitals.

The electronic structures of the complexes are clearly modulated by replacement of chloride by Cp. In the mono-Cp-TEMPO complex, the Cl 3p character (per Ti−Cl bond) and metal 4p character are reduced relative to $TiCl_3$TEMPO. The decrease in Cl 3p character is attributed to the strong donation of the Cp ligand and the η^1-TEMPO ligands, which decreases the contribution of the remaining chlorides. The

Table 3. Change in Total Bonding Energy for Replacement of Chloride by Cp

	ΔE (kcal/mol)
$TiCl_3TEMPO \rightarrow TiCpCl_2TEMPO$	−8.0
$TiCpCl_2TEMPO \rightarrow TiCp_2ClTEMPO$	+8.5
$Ti(III)Cl_3 \rightarrow Ti(III)CpCl_2$	−23.2
$Ti(III)CpCl_2 \rightarrow Ti(III)Cp_2Cl$	−15.7
$Ti(IV)Cl_3^+ \rightarrow Ti(IV)CpCl_2^+$	−47.2
$Ti(IV)CpCl_2^+ \rightarrow Ti(IV)Cp_2Cl^+$	−35.7
$Ti(IV)Cl_4 \rightarrow Ti(IV)CpCl_3$	−15.0
$Ti(IV)CpCl_3 \rightarrow Ti(IV)Cp_2Cl_2$	−2.9

decrease in metal 4p character in the calculations is attributed to an interference effect with the strongly donating Cp ligand, which is experimentally observed in the decreased Ti K-pre-edge intensity (Figure 1, bottom). On going to the bis-Cp-TEMPO complex, the covalency per Ti−Cl bond and the total 4p contribution decrease further. In addition, the presence of a second Cp weakens the Ti−TEMPO bond. The weaker Ti−TEMPO bond in the bis-Cp-TEMPO complex could contribute to the ability of this complex to readily undergo Ti−O bond cleavage. To examine this issue further, the energetics of this reaction are explored below.

B. Energetics. Previous DFT studies (B3LYP/6-31G*) revealed that the Ti−O bond energy decreases from 56 to 43 to 17 kcal/mol on going from $TiCl_3TEMPO$ to $TiCpCl_2$-TEMPO to $TiCp_2ClTEMPO$, respectively.[8] An experimental estimate for the Ti−O bond energy of $TiCp_2ClTEMPO$ yielded a value of 25 kcal/mol, indicating that the B3LYP/6-31G* level of theory leads to an underestimate of the bond energy by ∼7−8 kcal/mol. Using total energies from geometry-optimized spin-unrestricted calculations (BP86, ADF basis set V) of the reactant and products of the homolysis reactions, we determine Ti−O bond energies of 72, 57, and 33 kcal/mol for $TiCl_3TEMPO$, $TiCpCl_2TEMPO$, and $TiCp_2ClTEMPO$, respectively. Though the calculated energies are somewhat higher,[38] the trends are very similar and indicate that the Ti−O bond energy decreases significantly as chloride ligands are replaced by cyclopentadienyl ligands. As discussed previously,[8] this may be due to a destabilization of the Ti−TEMPO complexes by ancillary ligation and/or preferential stabilization of the Ti(III) product. In an effort to illuminate the influence of the cyclopentadienyl ligand bonding as a function of ancillary ligand environments, we have examined the energy of stabilization due to replacement of a chloride by a Cp in the reactant and in the Ti(III) product. The results are summarized in Table 3. Replacement of the first chloride by Cp in $TiCl_3TEMPO$ results in a stabilization of −8.0 kcal/mol. However, the addition of the second Cp has a destabilizing effect, raising the energy by 8.0 kcal/mol. The Ti(III) products are stabilized to a much greater extent. Replacement of a chloride by Cp in $Ti(III)Cl_3$ decreases the energy by −23.2 kcal/mol. The replacement of the second Cp by chloride has a smaller but still significant stabilization effect (−15.7 kcal/mol). These energetics argue that the homolysis reaction is dominantly driven by stabilization of the Ti(III) product with a smaller contribution due to destabilization of the bis-Cp-TEMPO reactant.

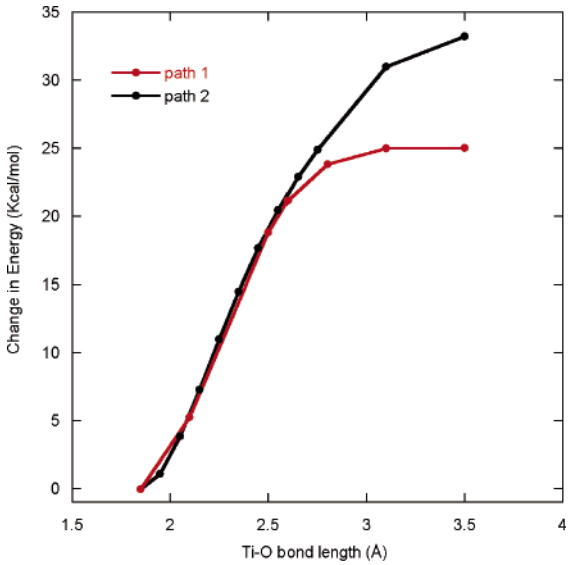

Figure 7. Calculated reaction coordinate for the homolytic cleavage of $TiCp_2ClTEMPO$ both with (path 1) and without (path 2) allowing for spin polarization.

To explore whether it is the Ti(III) oxidation state or the coordinatively unsaturated nature of the product that dominates the stabilization of the homolysis reaction, we have also explored the energetics of replacing chloride by Cp in Ti(IV) complexes with either three or four donor ligands. In a hypothetical three-coordinate $Ti(IV)Cl_3^+$ complex, replacement of a chloride by a Cp provides −47 kcal/mol of stabilization and replacement of a second chloride by Cp results in an additional −35.7 kcal/mol, indicating that a Ti(IV) complex with three donor ligands is stabilized by Cp more than the analogous Ti(III) complex. For four-coordinate $Ti(IV)Cl_4$, replacement of chloride by Cp results in −15 kcal/mol of stabilization and the second Cp results in only −3 kcal/mol. These results indicate that Cp provides a greater stabilizing effect when there are fewer donors to titanium.[39] Hence, these results indicate that the homolysis product of the bis-Cp-TEMPO complex is stabilized, not because it is Ti(III) but because it is a coordinatively unsaturated product.

C. Reaction Coordinate. DFT calculations were also used to examine the reaction coordinate of Ti−O bond homolysis in $TiCp_2ClTEMPO$. Since $TiCp_2ClTEMPO$ is known to cleave homolytically, at some point as the Ti−O bond is elongated (as the TEMPO is moved away from the $TiCp_2Cl$ fragment), spin polarization must occur. Spin-unrestricted DFT calculation were carried out both with (path 1, Figure 7) and without (path 2, Figure 7) spin polarization in order to determine its contribution to the energetics. A broken symmetry formalism in which the initial potentials of titanium and oxygen were modified was used to allow for

(38) This is most likely due to the use of the BP86 functional in this case vs the use of B3LYP/6-31G in ref 8. The hybrid functional will generally result in less covalent bonding and thus lower energies.

(39) It is also possible that the chloride is a poorer donor in three-coordinate environments. However, DFT calculations show that, in both Ti(IV) Cl_4 and Ti(IV) Cl_3^+, the covalency per Ti−Cl bond is ∼37%. In contrast, comparison of Ti(IV) $CpCl_3$ and Ti(IV) $CpCl_2^+$ shows that the total Ti−Cp character increases from 51% to 55%.

spin polarization. Figure 7 shows a plot of the total change in energy for these two pathways upon elongation of the Ti−O bond. The two paths are energetically very similar for Ti−O bond distance of 1.85−2.5 Å, showing no significant evidence for spin polarization. The two paths begin to deviate when the Ti−O bond is increased to a distance of 2.6 Å. At this point, path 1 shows the first evidence for significant spin polarization. There is an increase in positive spin density on the Ti (by 0.55 spins) and a negative spin density on TEMPO (by 0.52 spins). At a Ti−O distance of 3.1 Å, the spin density on the Ti increases to almost 1 full spin with a corresponding negative spin density on the TEMPO ligand. At this point, path 1 is ∼7 kcal/mol lower in energy then path 2. Since the total charge on the $TiCp_2Cl$ and TEMPO fragments is approximately equal (within 0.04 units) in both paths, the stabilization of path 1 relative to path 2 is attributed to the spin polarization.

As the Ti−O bond in $TiCp_2ClTEMPO$ is known to cleave homolytically, reduced charge separation must also play a role in stabilization of the products. The contribution of charge separation can be estimated from fragment calculations on the hypothetical heterolytic cleavage of $TiCp_2ClTEMPO$, which show this reaction to be uphill by ∼172 kcal/mol (for fragment calculations in a vacuum). Inclusion of benzene solvent in the fragment calculations lowers the Ti−O bond cleavage energy to ∼114 kcal/mol. However, this is still significantly greater than the Ti−O bond energy for the homolytic cleavage reaction (∼33 kcal/mol for fragment calculations in a vacuum and ∼24 kcal/mol in benzene) and indicates a significant contribution due to charge separation.

V. Summary

The results of both the Ti K- and Cl K-edge data on Ti complexes of known oxidation state have been used to establish the changes in pre-edge energies which result from oxidation of titanium. Comparison of the Ti K- and Cl K-edge XAS for the Ti−TEMPO series clearly shows that these complexes are described as Ti(IV)−TEMPO anion complexes. Further, the Cl K-edges show that the Ti−Cl bonding interaction has decreased on going from $TiCl_3TEMPO$ to $TiCpCl_2TEMPO$ to $TiCp_2ClTEMPO$, demonstrating that Cp is a strong donor that can decrease the interaction of titanium with the "spectator" chloride ligands.

The experimental data strongly correlate to DFT results at the GGA level. The excellent agreement with the DFT predicted Ti K- and Cl K-edge spectra allow for additional insights from the electronic structure calculations. The results show that on going from the mono-Cp-TEMPO to the bis-Cp-TEMPO the Ti−O bond is significantly weakened, demonstrating a spectator ligand effect similar to that observed for the chloride ligands. Although this is one factor that contributes to the homolysis of the Ti−O bond in the bis-Cp-TEMPO complex, the stabilization of the three-coordinate product by Cp makes a more significant contribution to the energetics. This stabilization results from the coordinative unsaturation rather than the Ti(III) nature of the product. Additional stabilization of the homolytic cleavage reaction derives from spin polarization and reduced charge separation along the reaction coordinate.

Acknowledgment. SSRL operations are funded by the Department of Energy, Office of Basic Energy Sciences. The Structural Molecular Biology program is supported by the National Institutes of Health, National Center for Research Resources, Biomedical Technology Program and by the Department of Energy, Office of Biological and Environmental Research.

Supporting Information Available: Ti K-edge data over the full edge region; geometry-optimized coordinates of $TiCl_3TEMPO$, $TiCpCl_2TEMPO$, $TiCp_2ClTEMPO$, and $Ti(Cp)_2Cl$. This material is available free of charge via the Internet at http://pubs.acs.org.

IC060402T